THE JOURNAL OF PHYSICAL CHEMISTRY B

ARTICLE

pubs.acs.org/JPCB

Electron-Transfer Reactions between the Diamagnetic Cation of α-Tocopherol (Vitamin E) and β-Carotene

Ying Shan Tan and Richard D. Webster*

Division of Chemistry and Biological Chemistry, School of Physical and Mathematical Sciences, Nanyang Technological University, Singapore 637371

Supporting Information

ABSTRACT: β-Carotene (β-Car) was chemically oxidized in a $-2e^-$ process using 2 mol equiv of $NOSbF_6$ in a 4:1 ratio (v/v) of dichloromethane:acetonitrile to form the β-carotene dication (β-Car^{2+}). Voltammetric monitoring of the chemical oxidation experiments over a range of temperatures indicated that the half-life of β-Car^{2+} was approximately 20 min at −60 °C, and approximately 1 min at −30 °C. α-Tocopherol (α-TOH) was chemically oxidized in a $-2e^-/-H^+$ process using 2 mol equiv of $NOSbF_6$ to form the diamagnetic cation (α-TO^+) which survives indefinitely at −60 °C in a 4:1 ratio (v/v) of dichloromethane:acetonitrile. Cyclic voltammetry experiments indicated that the oxidative peak potential for α-TOH was approximately +0.4 V more positive than the oxidative peak potential of β-Car. When solutions of α-TO^+/H^+ (prepared by chemical oxidation of α-TOH with 2 NO^+) were reacted with solutions containing equal molar amounts of β-Car, voltammetric monitoring indicated that α-TOH was quantitatively regenerated and β-Car^{2+} was formed in high yield in a homogeneous two-electron transfer, according to the reaction α-$TO^+ + H^+ + \beta$-Car → α-TOH + β-Car^{2+}.

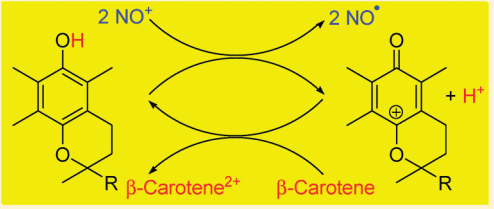

1. INTRODUCTION

α-Tocopherol (α-TOH), the most biologically active form of vitamin E, and β-carotene (β-Car) are produced by plants and when consumed by mammals reside inside the lipid bilayer membranes in living cells.[1] The widely accepted view is that α-TOH's major function in mammalian tissues is as an antioxidant, essentially a sacrificial compound that prevents cell membranes from turning rancid and decomposing.[2−4] An alternative, although less accepted view, is that α-TOH has a specific role as a cellular signaling molecule, and its antioxidant properties are of secondary or little importance biologically.[5−8] It is interesting to note that while α-TOH does unquestionably have antioxidant properties by virtue of its labile hydrogen atom on its hydroxyl group, many of the potential antioxidant benefits of consuming large doses of vitamin E are not realized in clinical trials.[9] Therefore, the nonantioxidant functions of α-TOH are attracting increasing interest.[10]

β-Car has an important dual role in nature as a photoprotecting agent and a light-harvesting antenna.[11] β-Car's main function in humans is as a pro-vitamin, where it converts into vitamin A via an enzymatic process in the intestines, although it has been reported that it also displays antioxidant properties.[12] A pulse radiolysis study initially concluded that the oxidized form of α-TOH (α-$TO^•$) could react with β-Car (plus a proton) to form the radical cation (β-$Car^{•+}$), thereby regenerating α-TOH (eq 1).[13] However, a following EPR study indicated that reaction 1 was unlikely to occur.[14] Therefore, a subsequent pulse radiolysis studied investigated the interactions between the one-electron-oxidized form of α-TOH (α-$TOH^{•+}$) and β-Car, and it was suggested that β-Car can regenerate α-TOH from its one-electron-oxidized form (eq 2).[15]

$$\alpha\text{-TO}^• + \beta\text{-Car} + H^+ \rightarrow \alpha\text{-TOH} + \beta\text{-Car}^{•+} \quad \text{(unlikely reaction)} \tag{1}$$

$$\alpha\text{-TOH}^{•+} + \beta\text{-Car} \rightarrow \alpha\text{-TOH} + \beta\text{-Car}^{•+} \tag{2}$$

The reaction in eq 2 is certainly electrochemically feasible based on the observation that α-$TOH^{•+}$ is a powerful enough oxidant to oxidize β-Car. Nevertheless, electrochemical studies have demonstrated that α-TOH[16−29] and β-Car[30−34] normally undergo two-electron oxidation at electrode surfaces in aprotic organic solvents such as CH_3CN and CH_2Cl_2. Therefore, this study is directed at determining whether a homogeneous two-electron reaction can occur between oxidized α-TOH and neutral β-Car.

The electrochemical oxidation mechanism for α-TOH in acetonitrile[16,17,19−28] and dichloromethane[17,20] is given in Scheme 1. α-TOH is initially oxidized by one electron to form the radical cation (α-$TOH^{•+}$). α-$TOH^{•+}$ rapidly loses a proton to form the neutral radical (α-$TO^•$), which is then immediately oxidized by one-electron at the electrode surface to form the diamagnetic cation (α-TO^+). Although the mechanism occurs in two one-electron steps, only one oxidative peak (E_p^{ox}) is observed during cyclic voltammetry experiments because the second electron-transfer step occurs at a lower (more negative) potential than the first electron-transfer step.[23] α-TOH can be quantitatively

Received: January 3, 2011
Revised: February 20, 2011
Published: March 18, 2011

Scheme 1. Electrochemically Induced Transformations of α-Tocopherol in CH_3CN or CH_2Cl_2[19] [a]

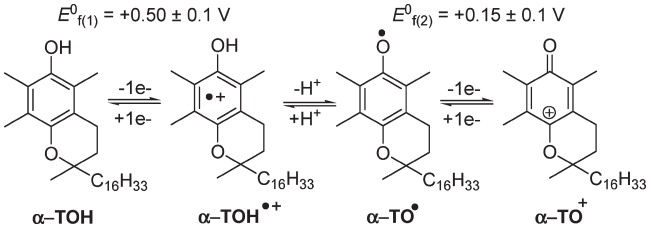

[a] One resonance structure is displayed for each compound. The counterions for the charged species are the supporting electrolyte anion [PF_6^-], and the "H^+" ions likely exist coordinated to the organic solvent (or with trace water). Formal potentials (E_f^0) are vs ferrocene/ferrocene$^+$ at 22 ± 2 °C.

regenerated from α-TO^+ on the milliseconds and hours time scales by applying a reducing potential to the electrode surface. The reaction in Scheme 1 is given as an ECE mechanism, where E represents an electron transfer at an electrode surface and C represents a homogeneous chemical step. However, it is uncertain whether the second electron-transfer step occurs via a heterogeneous electron transfer as given in Scheme 1 or by a homogeneous disproportionation mechanism.[25,35] It has been found that chemical oxidation of α-TOH with 2 mol equiv of NO^+ leads to α-TO^+ in 100% yield (eq 3).[20,28]

$$\alpha\text{-TOH} + 2NO^+SbF_6^- \rightarrow \alpha\text{-}TO^+SbF_6^- + H^+SbF_6^- + 2NO(g) \quad (3)$$

The free proton that is shown in Scheme 1 and eq 3 is released from the hydroxyl group during the forward oxidation step.[16,17,19] It has been assumed that the same proton is involved in protonating the phenoxyl when the diamagnetic cation (α-TO^+) is reduced back to the starting material via the phenoxyl radical (α-$TO^•$).[19−29] If a dry organic soluble acid such as CF_3SO_3H or CF_3COOH is added to the organic solvent, the lifetime of the radical cation (α-$TOH^{•+}$) increases substantially, resulting in the electrochemical oxidation occurring via one-electron (rather than two electrons when the oxidation is conducted in the absence of added acid).[17,19,21] Spectroscopic experiments (EPR, UV−vis, and FTIR) have shown that α-$TOH^{•+}$ can survive for at least several minutes at room temperature when produced in CH_3CN or CH_2Cl_2 containing strong organic acids.[17,19,21] However, such a strong acid environment is unlike any conditions that the compound is likely to experience in its natural lipophilic environment.

The electrochemical oxidation of β-Car occurs in two one-electron steps to first form the cation radical (β-$Car^{•+}$) and then the dication (β-Car^{2+}) (Scheme 2).[30−34] Detailed voltammetric analysis and quantum mechanical calculations have indicated that the second electron-transfer step most likely occurs at a less positive potential than the first electron-transfer step, although the potentials are very close.[34] Thus, cyclic voltammograms of β-Car in dichloromethane only display one forward oxidative peak (E_p^{ox}) associated with a two-electron transfer, and one reverse reductive peak (E_p^{red}) also corresponding to a two-electron transfer. Unlike α-TO^+ which is indefinitely long-lived in dry acetonitrile or dichloromethane, β-Car^{2+} only survives for a few seconds at room temperature in dichloromethane and undergoes a number of homogeneous chemical reactions to form largely unidentified products.[33]

Scheme 2. Electrochemical Oxidation Mechanism for β-Car in CH_2Cl_2[34] [a]

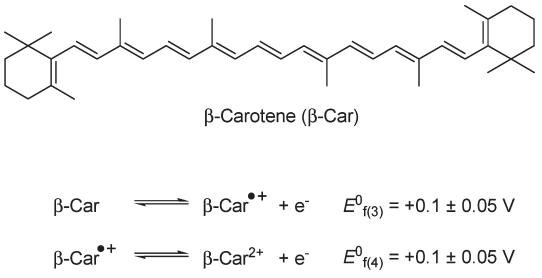

[a] Formal potentials (E_f^0) are vs ferrocene/ferrocene$^+$ at 22 ± 2 °C.

2. EXPERIMENTAL SECTION

2.1. Chemicals. (±)-α-TOH (97%) was obtained from Sigma-Aldrich and stored in the dark under nitrogen, and β-carotene (>97%) was obtained from TCI Japan and stored in the dark at 4 °C. $NOSbF_6$ (99%) used for chemical oxidation experiments was obtained from Sigma-Aldrich and stored in a glovebox in a nitrogen atmosphere. Bu_4NPF_6 was prepared by reacting equal molar amounts of aqueous solutions of Bu_4NOH (40%, Alfa Aesar) and HPF_6 (65%, Fluka), washing the precipitate with hot water, and recrystallizing 3 times from hot ethanol followed by drying under vacuum at 160 °C for 24 h and storing under vacuum. Molecular sieves of the form $^1/_{16}$ in. rods with 3 Å pore size (CAS 308080-99-1) were obtained from Fluka and all solvents were HPLC or analytical grade and used directly from the bottles (after drying over 3 Å molecular sieves).

2.2. Voltammetry. Cyclic voltammetry (CV) experiments were conducted with a computer-controlled Metrohm Autolab PGSTAT302N potentiostat. The working electrode was a 1 mm diameter Pt disk (Cypress Systems), used in conjunction with a Pt auxiliary electrode (Metrohm) and an Ag wire miniature reference electrode (Cypress Systems) connected to the test solution via a salt bridge containing 0.5 M Bu_4NPF_6 in CH_3CN. The internal filling solution of the reference electrode was prepared immediately prior to use to reduce the amount of contamination from water in the reference electrode filling solution. Accurate potentials were obtained using ferrocene as an internal standard. Rotating disk electrode (RDE) experiments were conducted with a Metrohm Autolab RDE-2 with a 3 mm diameter planar Pt electrode. Variable-temperature experiments were performed in a Metrohm jacketed glass cell with the temperature controlled with a Julabo FP89-HL ultralow refrigerated circulator and with a Thermo Electron Neslab RTE 740 circulating bath. UV−vis spectra were obtained with a Perkin-Elmer Lambda 750 spectrophotometer.

2.3. Measurement of Water Content of Organic Solvents. Karl Fischer (KF) titrations were conducted with a Mettler Toledo DL32 coulometer using (Riedel-deHaën) HYDRANAL-Coulomat CG for the cathode compartment. For the acetonitrile, Hydranal-coulomat AG was used for the anode compartment, while dichloromethane required HYDRANAL-Coulomat A for improved solubility. The water content of the solvents under experimental conditions was estimated by KF titrations to be $<10 \times 10^{-3}$ M.[36]

3. RESULTS AND DISCUSSION

3.1. Cyclic Voltammetry of α-TOH and β-Car in Mixed CH_2Cl_2/CH_3CN solutions. A method that enables likely

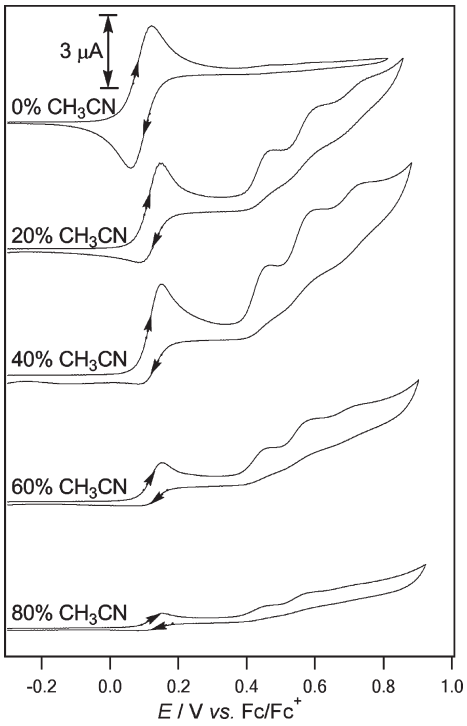

Figure 1. CVs of 1×10^{-3} M β-Car in CH_2Cl_2 containing 0.2 M Bu_4NPF_6 at 22 ± 2 °C recorded at a 1 mm diameter Pt electrode at a scan rate of 0.1 V s^{-1} with increasing percentages of CH_3CN. Positive current is in the upward direction.

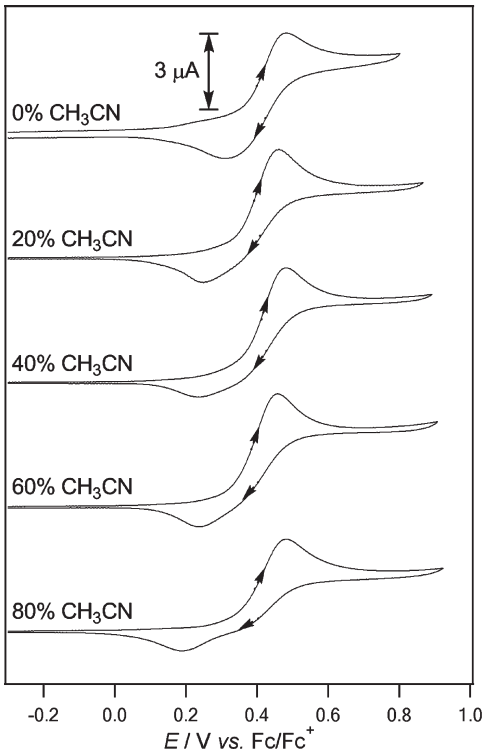

Figure 2. CVs of 1×10^{-3} M α-TOH in CH_2Cl_2 containing 0.2 M Bu_4NPF_6 at 22 ± 2 °C recorded at a 1 mm diameter Pt electrode at a scan rate of 0.1 V s^{-1} with increasing percentages of CH_3CN. Positive current is in the upward direction.

reactions between α-TO^+ and β-Car to be monitored involves preparing bulk solutions of α-TO^+ (that is known to be long-lived in low moisture content solvents[20,22]) and adding them to solutions containing β-Car, and monitoring the reaction products voltammetrically. Although α-TO^+ can be prepared by bulk controlled potential electrolysis of α-TOH,[19] a simpler method is via chemical reaction of α-TOH with 2 mol equiv of $NO^+SbF_6^-$ (eq 3).[20] Chemical oxidation was deemed preferable to electrochemical oxidation in an electrolysis cell because the chemical oxidation reaction occurs rapidly in 100% conversion and because it is easier to maintain the reaction solution in a low water content environment.[22] However, $NOSbF_6$ is poorly soluble in CH_2Cl_2 but very soluble in CH_3CN, while β-Car is insoluble in CH_3CN but reasonably soluble in CH_2Cl_2. Therefore, initial voltammetric experiments were performed by varying the amount of CH_2Cl_2 and CH_3CN to find a ratio where all the reagents were fully soluble.

Figure 1 show CVs of β-Car in CH_2Cl_2 at 22 ± 2 °C with increasing amounts of CH_3CN added. In pure CH_2Cl_2, the CV consists of a forward oxidation peak (E_p^{ox}) and a reverse reduction peak (E_p^{red}) separated by approximately 70 mV with a midpotential ($[E_p^{ox} + E_p^{red}]/2$) = +0.1 V vs Fc/Fc^+. The process corresponds to the chemically reversible two-electron oxidation of β-Car into β-Car^{2+} in two indistinguishable one-electron steps.[30−34] When the CH_2Cl_2 contained 20% CH_3CN, there was a decrease in the chemical reversibility of the oxidation process of β-Car (at a scan rate of 0.1 V s^{-1}), shown by how the anodic (i_p^{ox}) to cathodic (i_p^{red}) peak current ratio (i_p^{ox}/i_p^{red}) increased to ≫unity. Additional oxidation processes also became evident at potentials more positive than +0.4 V vs Fc/Fc^+ when CH_3CN was added to the CH_2Cl_2, associated with reaction products formed due to increased chemical instability (or reactivity) of β-Car^{2+} in the presence of CH_3CN. Furthermore, when the amount of CH_3CN was increased above 40%, the i_p^{ox} value associated with the two-electron oxidation of β-Car decreased substantially, due to insolubility of the β-Car.

CVs of α-TOH recorded under the same conditions as β-Car are shown in Figure 2. The CVs consist of a forward oxidation peak (E_p^{ox}) at approximately +0.5 V vs Fc/Fc^+ and a reverse reductive peak (E_p^{red}) at between +0.35 to +0.2 V vs Fc/Fc^+. The reverse reductive peak shifted to more negative potentials as increasing amounts of CH_3CN were added to the solution. The E_p^{ox} and E_p^{red} processes are associated with the forward and reverse reactions, respectively given in Scheme 1, and are due to the chemical reversible transformation of α-TOH into α-TO^+.[19,23] The reason for the wide separation between the E_p^{ox} and E_p^{red} values is because the two one-electron-transfer steps occur at different potentials with a proton-transfer reaction interspersed between the electron transfers (an ECE mechanism) (Scheme 1). The potentials given in Scheme 1 were estimated by digital simulation techniques at 22 ± 2 °C and are difficult to measure experimentally because the coupled proton-transfer reaction shifts the peaks away from the formal potentials.[25] The potentials are also influenced by the temperature and interactions of the phenol (α-TOH) with trace water in the solvent.

By comparing the results in Figures 1 and 2, it can be seen that α-TOH is more difficult to oxidize than β-Car by approximately +0.4 V (based on the E_p^{ox} values). Therefore, it would be expected that β-Car should be a sufficiently strong reductant to reduce α-TO^+ back to α-TOH (providing protons are available) and thereby be simultaneously oxidized to β-Car^{2+}. However, the prediction is uncertain because the second electron-transfer

dx.doi.org/10.1021/jp2000333 |J. Phys. Chem. B 2011, 115, 4244–4250

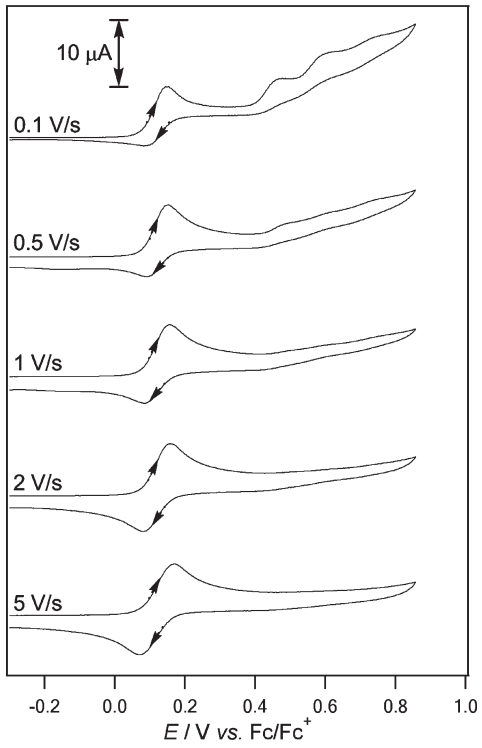

Figure 3. CVs of 1×10^{-3} M β-Car in CH_2Cl_2/CH_3CN (4:1) containing 0.2 M Bu_4NPF_6 at 22 ± 2 °C recorded at a 1 mm diameter Pt electrode at varying scan rates (ν). Positive current is in the upward direction. The current has been normalized by multiplying by $\nu^{-0.5}$.

step of α-TOH ($E^{o}_{f(2)}$ in Scheme 1) occurs at a much lower potential than the first electron-transfer step ($E^{o}_{f(1)}$). Therefore, the most reliable way to establish whether the reaction occurs is to prepare a solution of α-TO^+/H^+ and react it with β-Car and determine if α-TOH and β-Car^{2+} are indeed detected.

Because of the decreased lifetime of β-Car^{2+} in the presence of CH_3CN (Figure 1), it was decided to perform the chemical oxidation experiments in CH_2Cl_2 with 20% CH_3CN, which was high enough CH_3CN to enable the $NOSbF_6$ to fully dissolve but not to interfere in the solubility of β-Car. Figure 3 shows variable scan rate CVs of β-Car that were performed in CH_2Cl_2 containing 20% CH_3CN. It can be observed in Figure 3 that, as the scan rate approaches 5 V s^{-1}, the processes at potentials >+0.4 V vs Fc/Fc^+ decrease in intensity while simultaneously the reverse reduction peak at ~+0.05 V vs Fc/Fc^+ associated with the reduction of β-Car^{2+} back to β-Car increases in magnitude. Therefore, the variable scan rate CV experiments indicate that the lifetime of β-Car^{2+} is relatively short (≤1 s) at 22 ± 2 °C in CH_2Cl_2 containing 20% CH_3CN, since a scan rate of at least 5 V s^{-1} is needed to obtain an i_p^{ox}/i_p^{red} ratio equal to unity.

3.2. Measuring the Half-Life of β-Car^{2+} at Varying Temperatures in CH_2Cl_2/CH_3CN (4:1). The experiments shown in Figure 3 indicated that the lifetime of β-Car^{2+} is relatively short at room temperature. In order to increase the lifetime of β-Car^{2+} and thereby make it easier to detect after reacting β-Car with α-TO^+/H^+, experiments were performed at low temperatures by reacting β-Car with 2 mol equiv of $NOSbF_6$ in CH_2Cl_2/CH_3CN (4:1) (eq 4) and measuring the decay of β-Car^{2+} using square-wave voltammetry. The experiments were performed by adding 1 mL of a CH_3CN solution containing $NOSbF_6$ into 4 mL of a CH_2Cl_2 solution containing 1×10^{-3} M β-Car (and 0.2 M Bu_4NPF_6) and performing multiple square-wave voltammograms until the peak associated with the reduction of β-Car^{2+} could not be detected.

Table 1. First-Order Half-Life of β-Car^{2+} (Produced According to Eq 4) Measured by Square-Wave Voltammetry in Dichloromethane/Acetonitrile (4:1) Containing 0.2 M Bu_4NPF_6 at Various Temperatures[a]

temp/°C	half-life/min
−65	28.9
−60	19.3
−55	6.4
−50	2.6
−40	1.6
−30	1.2

[a] Kinetic plots are given in Figures S1 and S2 in the Supporting Information.

$$\beta\text{-Car} + 2NO^+SbF_6^- \rightarrow \beta\text{-}Car^{2+}(SbF_6^-)_2 + 2NO(g) \quad (4)$$

First-order kinetic plots obtained by observing the voltammetric decay of β-Car^{2+} are provided in the Supporting Information, and the estimated half-lives at a range of temperatures are given in Table 1. There are several studies that have measured the decay of neutral β-Car in a variety of matrixes that have suggested that the reactions do follow first-order kinetics.[37−40] However, the reaction products are complicated and it is possible that several competing pathways are involved. The results in Table 1 indicate that there is a substantial increase in the lifetime of β-Car^{2+} as the temperature decreases below −55 °C. At temperatures ≥ −30 °C, it was found that the loss of β-Car^{2+} occurred at a fast rate that could not be reliably measured by square-wave voltammetry, which accounts for the relatively large scatter in the kinetic plot at −30 °C in Figure S2 in the Supporting Information. The exact value of the half-life of β-Car^{2+} at different temperatures is not critical to this work, but based on the results in Table 1, it was concluded that, at a temperature of −60 °C, the lifetime of β-Car^{2+} was sufficiently long to be able to be easily observed voltammetrically as the major reaction product if formed via the reaction of β-Car with α-TO^+, without interference from other reaction products.

3.3. Reacting α-TO^+ with β-Car in CH_2Cl_2/CH_3CN (4:1) at −60 °C. Figure 4 shows CVs at a stationary electrode and linear sweep voltammograms (LSVs) using a rotating disk electrode (RDE) of β-Car and α-TOH in CH_2Cl_2/CH_3CN (4:1) containing 0.2 M Bu_4NPF_6 at −60 °C. Because of the very low temperature, both the CV and RDE experiments showed effects of distortion due to the high uncompensated solution resistance. In particular, there was a wide separation between the forward and reverse peaks during CV measurements and the waves detected during LSV measurements at the RDE were drawn out over a relatively wide potential range. Nevertheless, the shapes of the voltammetric waves were acceptable in the sense that the oxidation processes were clearly detected.

When CV experiments are performed at stationary electrodes, the oxidation state of the electroactive molecules present in the bulk solution can sometimes be difficult to determine, because the position of where zero current flow is observed can depend on where the potential scan is first commenced. In contrast, RDE experiments or measurements at microelectrodes always allow the position of zero current flow to be determined because new

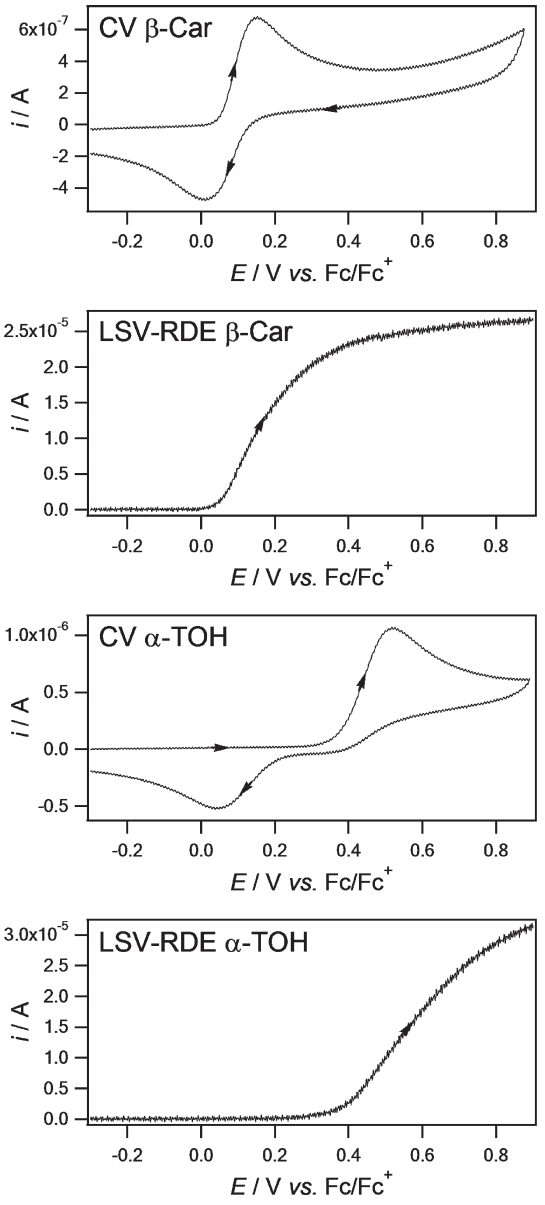

Figure 4. Voltammograms of 1×10^{-3} M β-Car or α-TOH in CH_2Cl_2/CH_3CN (4:1) containing 0.2 M Bu_4NPF_6 at −60 °C. CV experiments were performed in a stationary solution at a 1 mm diameter planar Pt electrode at a scan rate of 0.1 V s^{-1}, while RDE experiments were performed at a 3 mm diameter planar Pt RDE with a rotation speed of 2000 rpm at a scan rate of 0.05 V s^{-1}.

species from the bulk solution are continually being refreshed at the electrode surface. Therefore, the LSV-RDE experiments were performed as a method for determining the oxidation state of the molecules in solution immediately after the chemical oxidation experiments (reacting α-TO^+/H^+ with β-Car) were performed.

Figure 5 shows a LSV-RDE experiment when equal amounts of neutral α-TOH and β-Car are present in solution, with the voltammetric scan in the positive potential direction. At potentials <0 V vs Fc/Fc^+, no Faradaic current flows because the potential is not sufficiently high to oxidize β-Car or α-TOH. As the potential reaches +0.05 V vs Fc/Fc^+, β-Car begins to be oxidized and the current increases. When only β-Car is present in solution, a plateau is reached at approximately +0.5 V vs Fc/Fc^+ due to the convective-diffusion limited current (Figure 4).

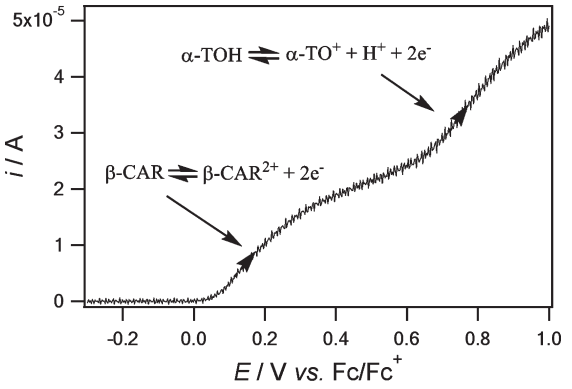

Figure 5. Linear sweep voltammogram of 1×10^{-3} M β-Car plus 1×10^{-3} M α-TOH in CH_2Cl_2/CH_3CN (4:1) containing 0.2 M Bu_4NPF_6 at −60 °C and recorded at a scan rate of 0.05 V s^{-1} at a 3 mm diameter planar Pt RDE with a rotation speed of 2000 rpm.

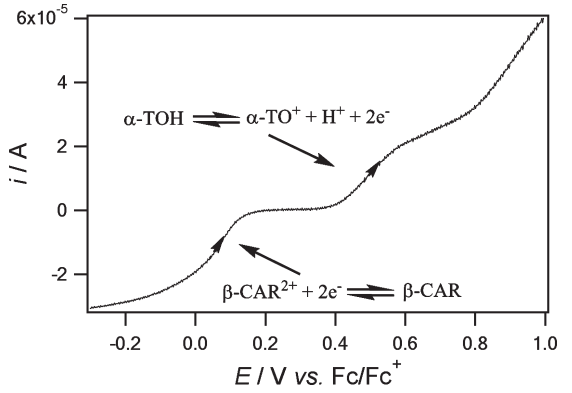

Figure 6. Linear sweep voltammogram obtained immediately (within 1 min) after combining 1×10^{-3} M β-Car with 1×10^{-3} M α-TO^+ in CH_2Cl_2/CH_3CN (4:1) containing 0.2 M Bu_4NPF_6 at −60 °C and recorded at a scan rate 0.05 V s^{-1} at a 3 mm diameter planar Pt RDE with a rotation speed of 2000 rpm.

However, in the presence of α-TOH, the current continues to rise due to the further oxidation of α-TOH at more positive potentials (Figure 5). It can be observed in Figure 5 that the oxidation process for α-TOH appears to shift to more positive potentials compared to when only α-TOH is present in solution (Figure 4). The reason for the apparent shift in potential most likely relates to a homogeneous reaction between α-TO^+/H^+ and β-Car in the bulk solution, which regenerates α-TOH, and which then undergoes oxidation again (eq 5).

$$\alpha\text{-TO}^+ + \text{H}^+ + \beta\text{-Car} \rightarrow \alpha\text{-TOH} + \beta\text{-Car}^{2+} \qquad (5)$$

Figure 6 shows an LSV-RDE experiment that was commenced within 30 s of adding a solution of α-TO^+/H^+ to a solution of β-Car at −60 °C. The experiment was performed by first reacting α-TOH with 2 mol equiv of NO^+ in CH_3CN at −40 °C to produce α-TO^+/H^+ (eq 3). Then 1 mL of the α-TO^+/H^+ solution was added to 4 mL of β-Car in CH_2Cl_2 at −60 °C, so that the concentration of both species was equal to 1×10^{-3} M. The voltammogram in Figure 6 shows that the position of zero current flow is between +0.2 and +0.4 V vs Fc/Fc^+. Therefore, it can be concluded that vitamin E exists in its neutral form

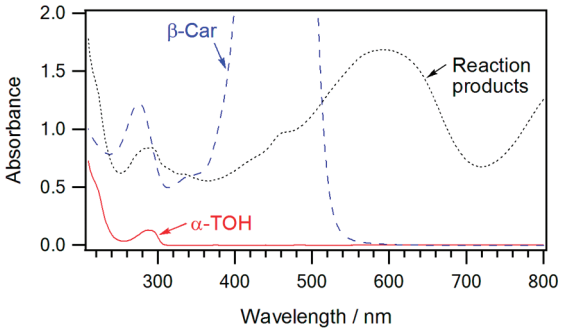

Figure 7. Background subtracted UV−vis spectra obtained in solutions of CH_2Cl_2/CH_3CN (4:1) in an approximately 0.5 mm path length quartz cell at 22 ± 2 °C: (—) 1×10^{-3} M α-TOH, (---) 1×10^{-3} M β-Car, and (···) the products of the reaction between 1×10^{-3} M α-TO^+/H^+ and 1×10^{-3} M β-Car according to eq 5.

(α-TOH) and β-Car has been oxidized to its dication (β-Car^{2+}), according to the forward reaction in eq 5. The H^+ given in eq 5 is released during the initial oxidation of α-TOH by 2 $NO^+SbF_6^-$ and most likely exists in solution bound to trace water or to the solvent molecules, and therefore, does not need to come from any other source.[22]

The kinetic data in Table 1 indicates that β-Car^{2+} survives at −60 °C for a much longer time than the time scale of the voltammetric experiment in Figure 6 (the LSV-RDE scan was completed in <1 min of mixing the solution of α-TO^+ and β-Car); therefore, the voltammetric data are not affected by the decay of β-Car^{2+}. Based on the magnitude of the limiting current values in Figure 6 and comparing them to the limiting current values recorded for equivalent concentrations of the individual neutral compounds under identical conditions (Figure 4), it is estimated that the transformation in eq 5 occurs in a very high yield (>90%).

The products of the reaction between α-TO^+/H^+ and β-Car were also measured by UV−vis spectroscopy after the solution was warmed to room temperature. Figure 7 (red line) shows the UV−vis spectrum of 1×10^{-3} M α-TOH in CH_2Cl_2/CH_3CN (4:1) which displays an absorbance at 295 nm with $\varepsilon = 3.4 \times 10^3$ L mol^{-1} cm^{-1}.[28,41] The UV−vis spectrum of solutions containing β-Car obtained under the same conditions and concentration as α-TOH displayed a strong absorbance at 276 nm and very strong absorbances between 360 and 560 nm (Figure 7, blue dashed line). The spectra in Figure 7 indicate that solutions containing β-Car absorb much more strongly than α-TOH over all wavelengths <600 nm. An additional UV−vis spectrum of β-Car at lower concentration is provided in the Supporting Information.

The black dotted line in Figure 7 is the UV−vis spectrum obtained after α-TO^+/H^+ was reacted with β-Car at −60 °C and then the solution allowed to warm to room temperature. The spectrum of the reaction products in Figure 7 (dotted black line) supports the reaction mechanism given in eq 5, where the α-TOH is regenerated from α-TO^+/H^+ and all of the β-Car converted into β-Car^{2+}. An absorbance band was detected at 295 nm (Figure 7, black dotted line) with a similar shape and intensity as expected for α-TOH (Figure 7, red line), taking into account that the background absorbance readings at all wavelengths <600 nm are much higher when β-Car and its reaction products are also present. Furthermore, the very intense bands associated with neutral β-Car between 360 and 560 nm are missing from the spectrum of the reaction products, indicating that all of the β-Car had reacted with α-TO^+/H^+, thereby supporting the quantitative reaction of α-TO^+/H^+ with β-Car in a two-electron process. At the higher temperature, the β-Car^{2+} is unstable/reactive and further reacts/decomposes to form other unknown products.

4. CONCLUSIONS

The results in this study have proven that β-Car is able to regenerate α-TOH from α-TO^+/H^+ in a $-2e^-$ homogeneous reaction to form β-Car^{2+} in high yield. The reaction was performed at low temperatures in order to stabilize the β-Car^{2+} for sufficiently long time to allow its unequivocal identification using linear sweep voltammetry at a rotating disk electrode. Future experiments at higher temperatures to determine the rate of reaction of α-TO^+/H^+ and β-Car are possible using stopped-flow measurements combined with UV−vis spectrophotometric detection, since both β-Car and α-TO^+ are long-lived in separate solutions (provided the moisture contents of the solvents are low).

■ ASSOCIATED CONTENT

Supporting Information. First-order kinetic plots of the decay of β-Car^{2+} at variable temperatures and UV−vis spectrum of β-Car. This material is available free of charge via the Internet at http://pubs.acs.org.

■ AUTHOR INFORMATION

Corresponding Author

*E-mail: webster@ntu.edu.sg. Tel.: +65 6316 8793. Fax: +65 6791 1961.

■ ACKNOWLEDGMENT

This work was supported by a Singapore Government Ministry of Education research grant (T208B1222).

■ REFERENCES

(1) *Biochemistry of Lipids, Lipoproteins and Membranes*, 4th ed.; Vance, D. E., Vance, I. E., Eds.; Elsevier: Amsterdam, 2002.
(2) Burton, G. W.; Ingold, K. U. *Acc. Chem. Res.* **1986**, *19*, 194–201.
(3) Bowry, V. W.; Ingold, K. U. *Acc. Chem. Res.* **1999**, *32*, 27–34.
(4) Traber, M. G.; Atkinson, J. *Free Radical Biol. Med.* **2007**, *43*, 4–15.
(5) Azzi, A. *Free Radical Biol. Med.* **2007**, *43*, 16–21.
(6) Boscoboinik, D.; Szewczyk, A.; Hensey, C.; Azzi, A. *J. Biol. Chem.* **1991**, *266*, 6188–6194.
(7) Tasinato, A.; Boscoboinik, D.; Bartoli, G.-M.; Maroni, P.; Azzi, A. *Proc. Natl. Acad. Sci. U.S.A.* **1995**, *92*, 12190–12194.
(8) Azzi, A.; Stocker, A. *Prog. Lipid Res.* **2000**, *39*, 231–255.
(9) Melton, L. *New Scientist* **2006**, *191*, 40–43.
(10) Brigelius-Flohé, R.; Davies, K. J. A. *Free Radical Biol. Med.* **2007**, *43*, 2–3.
(11) Koyama, Y. *J. Photochem. Photobiol.* **1991**, *B9*, 265–280.
(12) Burton, G. W.; Ingold, K. U. *Science* **1984**, *224*, 569–573.
(13) Böhm, F.; Edge, R.; Land, E. J.; McGarvey, D. J.; Truscott, T. G. *J. Am. Chem. Soc.* **1997**, *119*, 621–622.
(14) Valgimigli, L.; Lucarini, M.; Pedulli, G. F.; Ingold, K. U. *J. Am. Chem. Soc.* **1997**, *119*, 8095–8096.
(15) Edge, R.; Land, E. J.; McGarvey, D.; Mulroy, L.; Truscott, T. G. *J. Am. Chem. Soc.* **1998**, *120*, 4087–4090.

(16) Marcus, M. F.; Hawley, M. D. *Biochim. Biophys. Acta* **1970**, *201*, 1–8.
(17) Svanholm, U.; Bechgaard, K.; Parker, V. D. *J. Am. Chem. Soc.* **1974**, *96*, 2409–2413.
(18) Webster, R. D. *Electrochem. Commun.* **1999**, *1*, 581–584.
(19) Williams, L. L.; Webster, R. D. *J. Am. Chem. Soc.* **2004**, *126*, 12441–12450.
(20) Lee, S. B.; Lin, C. Y.; Gill, P. M. W.; Webster, R. D. *J. Org. Chem.* **2005**, *70*, 10466–10473.
(21) Wilson, G. J.; Lin, C. Y.; Webster, R. D. *J. Phys. Chem. B* **2006**, *110*, 11540–11548.
(22) Lee, S. B.; Willis, A. C.; Webster, R. D. *J. Am. Chem. Soc.* **2006**, *128*, 9332–9333.
(23) Webster, R. D. *Acc. Chem. Res.* **2007**, *40*, 251–257.
(24) Peng, H. M.; Webster, R. D. *J. Org. Chem.* **2008**, *73*, 2169–2175.
(25) Yao, W. W.; Peng, H. M.; Webster, R. D.; Gill, P. M. W. *J. Phys. Chem. B* **2008**, *112*, 6847–6855.
(26) Peng, H. M.; Choules, B. F.; Yao, W. W.; Zhang, Z.; Webster, R. D.; Gill, P. M. W. *J. Phys. Chem. B* **2008**, *112*, 10367–10374.
(27) Yao, W. W.; Peng, H. M.; Webster, R. D. *J. Phys. Chem. C* **2009**, *113*, 21805–21814.
(28) Chen, S.; Peng, H. M.; Webster, R. D. *Electrochim. Acta* **2010**, *55*, 8863–8869.
(29) Yao, W. W.; Lau, C.; Hui, Y.; Poh, H. W.; Webster, R. D. *J. Phys. Chem. C* **2011**, *115*, 2100–2113.
(30) Jeevarajan, J. A.; Jeevarajan, A. S.; Kispert, L. D. *J. Chem. Soc., Faraday Trans.* **1996**, *92*, 1757–1765.
(31) Jeevarajan, J. A.; Wei, C. C.; Jeevarajan, A. S.; Kispert, L. D. *J. Phys. Chem.* **1996**, *100*, 5637–5641.
(32) Kispert, L. D.; Gao, G.; Deng, Y.; Konovalov, V.; Jeevarajan, A. S.; Jeevarajan, J. A.; Hand, E. *Acta Chem. Scand.* **1997**, *51*, 572–578.
(33) Liu, D. Z.; Gao, Y. L.; Kispert, L. D. *J. Electroanal. Chem.* **2000**, *488*, 140–150.
(34) Hapiot, P.; Kispert, L. D.; Konovalov, V. V.; Saveant, J.-M. *J. Am. Chem. Soc.* **2001**, *123*, 6669–6677.
(35) Costentin, C. *Chem. Rev.* **2008**, *108*, 2145–2179.
(36) Hui, Y.; Webster, R. D. *Anal. Chem.* **2011**, *83*, 976–981.
(37) Mortensen, A.; Skibsted, L. H. *J. Agric. Food. Chem.* **2000**, *48*, 279–286.
(38) Wache, Y.; Bosser-DeRatuld, A.; Lhuguenot, J.-C.; Belin, J.-M. *J. Agric. Food. Chem.* **2003**, *51*, 1984–1987.
(39) Dutta, D.; Dutta, A.; Raychaudhuri, U.; Chakraborty, R. *J. Food. Eng.* **2006**, *76*, 538–546.
(40) Ferreira, J. E. M.; Rodriguez-Amaya, D. B. *J. Food. Sci.* **2008**, *78*, C589–C594.
(41) Naqvi, K. R.; Li, H.; Melø, T. B.; Zhang, Y.; Webster, R. D. *J. Phys. Chem. A* **2010**, *114*, 10795–10802.